ISSN 1674-1056
http://cpb.iphy.ac.cn
http://iopscience.iop.org/cpb
中国物理 B
Chinese Physics
中国物理
Chinese Physics B

Particle swarm optimization and its application to the design of a compact tunable guided-mode resonant filter

Dan-Yan Wang(王丹燕), Qing-Kang Wang(王庆康)
Citation: Chin. Phys. B . 2018, 27(3): 037801. **doi:** 10.1088/1674-1056/27/3/037801

Journal homepage: http://cpb.iphy.ac.cn; http://iopscience.iop.org/cpb

What follows is a list of articles you may be interested in

Semi-analytical method of calculating the electrostatic interaction of colloidal solutions

Hongqing Tian(田洪庆), Zengju Lian(连增菊)
Chin. Phys. B . 2017, 26(1): 017801. **doi:** 10.1088/1674-1056/26/1/017801

Temperature dependent direct-bandgap light emission and optical gain of Ge

Zhi Liu(刘智), Chao He(何超), Dongliang Zhang(张东亮), Chuanbo Li(李传波), Chunlai Xue(薛春来), Yuhua Zuo(左玉华), Buwen Cheng(成步文)
Chin. Phys. B . 2016, 25(5): 057804. **doi:** 10.1088/1674-1056/25/5/057804

Wavelength modulation spectroscopy at 1530.32 nm for measurements of acetylene based on Fabry-Perot tunable filter

Yun-Long Li(李运龙), Bing-Chu Yang(杨兵初), Xue-Mei Xu(许雪梅)
Chin. Phys. B . 2016, 25(2): 024208. **doi:** 10.1088/1674-1056/25/2/024208

Vibration analysis of a new polymer quartz piezoelectric crystal sensor for detecting characteristic materials of volatility liquid

Gu Yu, Li Qiang, Xu Bao-Jun, Zhao Zhe
Chin. Phys. B . 2014, 23(1): 017804. **doi:** 10.1088/1674-1056/23/1/017804

Optical study of $Ba(Mn_xTi_{(1-x)}O_3)$ thin films by spectroscopic ellipsometry

Zhang Ting, Yin Jiang, Ding Ling-Hong, Zhang Wei-Feng
Chin. Phys. B . 2013, 22(11): 117801. **doi:** 10.1088/1674-1056/22/11/117801

Particle swarm optimization and its application to the design of a compact tunable guided-mode resonant filter*

Dan-Yan Wang(王丹燕) and Qing-Kang Wang(王庆康)†

Key Laboratory for Thin Film and Micro-fabrication of the Ministry of Education, Department of Microelectronics and Nanoscience, Shanghai Jiao Tong University, Shanghai 200240, *China*

(Received 14 October 2017; revised manuscript received 7 December 2017; published online 13 February 2018)

A compact tunable guided-mode resonant filter (GMRF) in the telecommunication region near the 1550 nm wavelength is proposed in this paper. Particle swarm optimization (PSO) is used to design the GMRF. The tunability of the GMRF is achieved by an MEMS-based physical movement (in the horizontal or vertical direction) combined with an incident angle in a certain range. The results show that the resonant wavelength tuning of 110 nm (140 nm) is obtained by horizontal movement of 168 nm (vertical movement of 435 nm) combined with an about 11° variation of incident angle.

Keywords: guided-mode resonant filter (GMRF), particle swarm optimization (PSO), tunable filter, rigorous coupled wave analysis (RCWA)

PACS: 78.20.Bh, 78.20.Ci, 42.25.Fx **DOI:** 10.1088/1674-1056/27/3/037801

1. Introduction

Guided-mode resonant filter (GMRF) has received more and more attention recently because of its distinct advantages, such as high diffraction efficiency, narrow band, spectral or color sensitivity, etc.[1–6] Particularly, GMRF with subwavelength grating is of the most interest for the ability to concentrate the energy, allowing only 0^{th}-order propagation.[7]

One of the important and desirable features of the GMRF is its resonance tunability. The characteristics of the resonance tuning are dependent on several parameters, including the grating period, layer thickness, incident angle, refractive index of the material, and surrounding media. Therefore, a tunable GMRF device can be achieved by controlling these parameters. Uddin experimentally demonstrated an angle-tuned GMRF color filter, which exhibited blue, green and red color responses at incident angles of 8°, 20°, and 35°, respectively.[8] One year later, he designed and fabricated a highly efficient tunable filter for three different grating periods.[9] Sang *et al.* proposed a novel bandwidth tunable GMRF based on a contact coupled gratings with the absentee layers at oblique incidence.[10] Lin and Huang fabricated and characterized a linear variable filter based on a GMRF with gradient grating periods.[11] A tunable GMRF for incident wave with arbitrary polarization was achieved by placing two identical waveguide gratings close to and their grooves perpendicular to each other.[12] There were also a few tunable GMRF devices proposed by utilizing electro-optic effect[13,14] and thermo-optic effect.[15] Furthermore, MEMS-based GMRF can also achieve the tunable functionality. For example, a tunable double-grating resonant leaky mode microelectromechanical-type element was proposed by Magnusson and Ding in 2006,[16] in which a significant level of tunability was demonstrated by adjusting mechanically the structural symmetry of the grating profile; an MEMS-tunable leaky mode structure had been investigated for applications in multispectral and hyperspectral imaging.[17] However, the structures mentioned above are complex, which will increase the difficulty in manufacturing and cost.

In this paper, a compact tunable GMRF in the telecommunication region near the 1550 nm wavelength is proposed, and particle swarm optimization (PSO) method is used to design this structure since it is a robust, stochastic evolutionary strategy. The designed tunable GMRF is achieved by an MEMS-based motion in the horizontal and vertical direction combined with an incident angle in a certain range. It should be noted that the MEMS operation and design are both out of scope of our work and only tuning by MEMS concept is treated in this paper.

2. Design methods

The proposed tunable GMRF consists of a subwavelength grating layer which is placed on a substrate as shown in Fig. 1. The Λ and d denote the period and thickness of the grating, respectively, n_{H} and n_{L} are the refractive indices of the materials in the grating region, respectively. Also, n_{c} and n_{S} refer to the refractive indices of the cover and substrate media. Classic incidence is the precondition in this paper as shown in Fig. 1(a), which means that the incident wave vector is in the xz plane with an azimuthal angle $\alpha = 0°$.[18] The θ is the incident angle measured from the z-axis in the plane of incidence. The polarization of the E vector is oriented in a polarization plane normal to the direction defined by K, where

*Project supported by the National High-Tech Research and Development Program of China (Grant No. 2011 AA050518).

†Corresponding author. E-mail: wangqingkang@sjtu.edu.cn

© 2018 Chinese Physical Society and IOP Publishing Ltd

$\varphi = 0°$ corresponds to the s-polarization and $\varphi = 90°$ is for the p-polarization. Here, we treat the case of an s-polarization incidence.

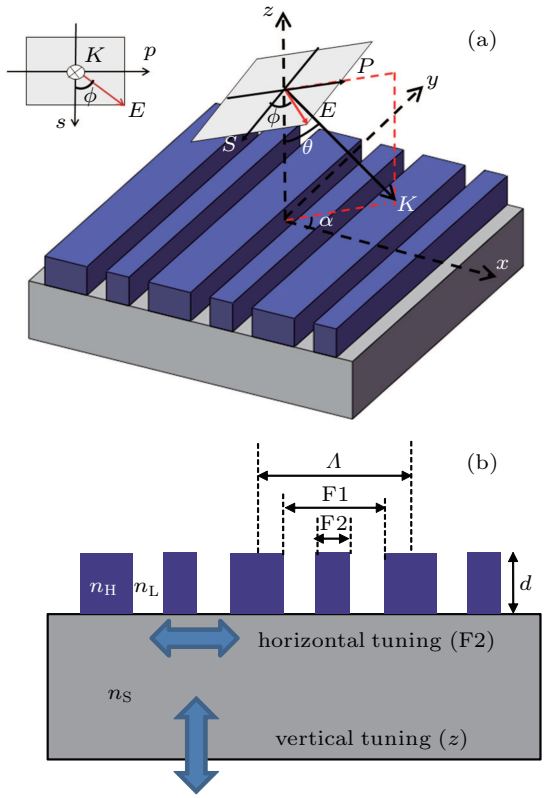


Fig. 1. (color online) Schematic structure of the tunable filter based on GMR effect, showing (a) three-dimensional view of the structure, and (b) cross sectional view of the element in the XZ plane, with the parameters of $n_H = 2.5$, $n_S = 1.4$, $n_L = n_c = 1$, and $\alpha = \varphi = 0°$.

One period of the grating layer is composed of a mobile fraction with fill factor F2 inside an air groove with fill factor F1 as illustrated in Fig. 1(b). In addition, F2 fraction attached to the substrate can be moved by the conceptual MEMS mechanism in two directions, horizontal and vertical. Meanwhile, the structural parameters of the GMRF, including the period and thickness of the grating, width of the mobile fraction F2 and air groove F1, remain constant in the moving process. The movement in the horizontal direction can lead to the variation in grating profile symmetry and the vertical movement can make alteration in the total grating layer thickness. As the substrate moves through MEMS actuators, the position of the F2 fraction in the structure changes, the distributions of the refractive index in the grating layer and the symmetry of the profile also change, and finally the location of the resonant wavelength on reflectance spectrum is varied.

In order to obtain optimal structural parameters, we choose the PSO method[19,20] to design this GMRF since it is a robust, stochastic evolutionary strategy and has been utilized in electromagnetic design problems. The basic solution process of the PSO can be divided into four steps as shown in Fig. 2.

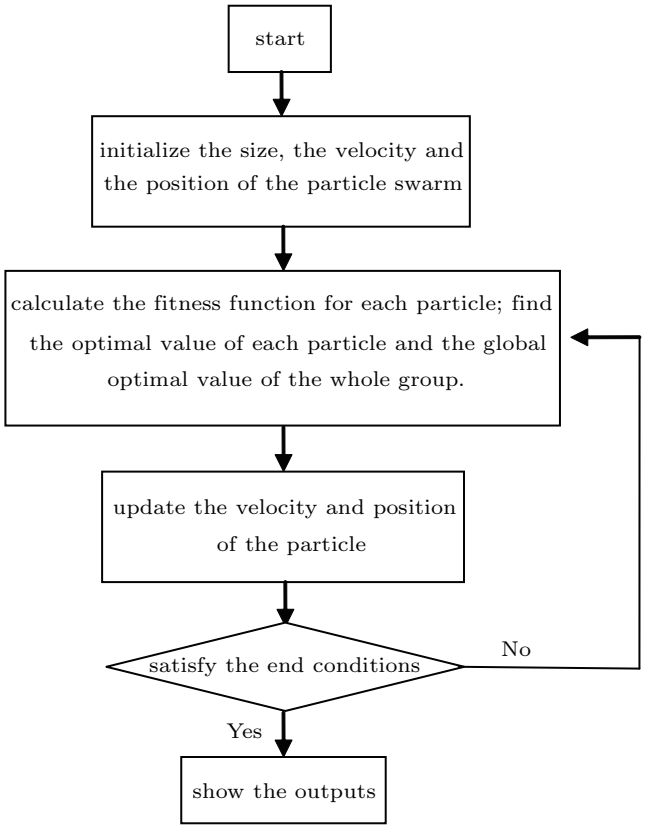


Fig. 2. Basic optimal steps of the PSO.

Firstly, we need to set the particle swarm size, the maximum velocity range, and the whole search space. The velocity V_m and position X_m of each particle can be randomly initialized in the velocity range and the whole search space. The period and thickness of the grating layer as well as the widths of F1 and F2 fractions need to be optimized in this paper. Thus, the dimension of the particle is 4. In addition, the number of particles in the swarm is set to be 20. Velocity is the rate of a particle's position change which is set to be between -1 and 1. The whole search spaces of the structural parameters, i.e., grating period, grating thickness, widths of F1 and F2 fractions are set to be 0.8–1.3 μm, 0.1–2.0 μm, 0.5–1.0 μm, and 0.1–0.5 μm, respectively, according to the resonant wavelength. Secondly, we need to calculate a fitness function (FF), the best previous particle position (P_{best}) and the position of the best particle in the swarm (G_{best}). The FF is defined and determined for each particle according to its optimization parameters in order to evaluate the quality of particles. Here, the FF is taken to be a root mean square (RMS) error function

$$\mathrm{FF} = \sqrt{\frac{1}{M}\sum_{\lambda_i}[R_{\mathrm{desired}}(\lambda) - R_{\mathrm{design}}(\lambda)]^2}, \tag{1}$$

where M is the number of the wavelength points, R_{desired} and R_{design} are the target reflection and the calculated reflection by PSO, respectively. Rigorous coupled-wave analysis (RCWA) is carried out for the calculating of the designed reflection. Forty-one wavelength points (i.e., $M = 41$) are used for FF

calculations and 21 diffraction orders are retained for analysis. The P_{best} is set initially to be the first random particle position P_{m}, and if FF(X_m^{k+1}) is better than FF(P_{m}), then $P_{\text{m}} = X_m^{k+1}$, where X_m^{k+1} is the particle position in $(k+1)$th iteration in step 3; G_{best} is kept as the best position G of the swarm, and if the best of FF(P_{m}) is better than FF(G), then G is the best of P_{m}.

In Step 3, we need to update the velocity and position. The particle position and velocity in $(k+1)$th iteration are modified as follows:

$$\begin{aligned} V_m^{k+1} &= \omega V_m^k + c_1 \text{rand}_1()(P_m - \text{X}_m^k) \\ &\quad + c_2 \text{rand}_2()(G - X_{\text{m}}^k), \\ X_m^{k+1} &= X_m^k + V_m^{k+1}\Delta t, \end{aligned} \tag{2}$$

where ω, c_1, and c_2 are the inertia weight, cognitive and social rates with the corresponding values of 0.5, 1.49, and 1.49, respectively. $\text{rand}_1()$ and $\text{rand}_2()$ are two uniformly distributed random numbers with values between 0 and 1. In addition, Δt is the time step, and we consider $\Delta t = 1.0$. Finally, the total iterations are set as the end condition: the calculate process will turn to step 2 if it cannot meet the given iterations; on the contrary, it will show the outputs if the given iterations are completed.

3. Results and discussion

The (x_1, y_1, z_1) is assumed to be the coordinate of the F2 fraction. Here the inner F2 fraction is considered to be in the middle of F1, with (x_1, y_1, z_1) being (0, 0, 0). For the design of GMRF with a normal incidence, four parameters need to be optimized by PSO: $\{\Lambda, d, \text{F1}, \text{F2}\}$. After 1000 iterations by PSO method with code written in MATLAB, FF of the best particle reduces to about 0.09 as illustrated in Fig. 3(a), with filter structure being {1 μm, 1.8799 μm, 0.876 μm, 0.1 μm}. Figure 3(b) demonstrates the reflectance spectra of the designed filter and a target which is a reflection filter (wavelength ranging from 1.45 μm to 1.65 μm) with $a \sim 5$ nm linewidth as indicated by the red dotted line in Fig. 3(b). A commercial software package (R-soft DiffractMOD) based on the rigorous coupled wave analysis method (RCWA) is used to model the optical responses of the designed GMRF.

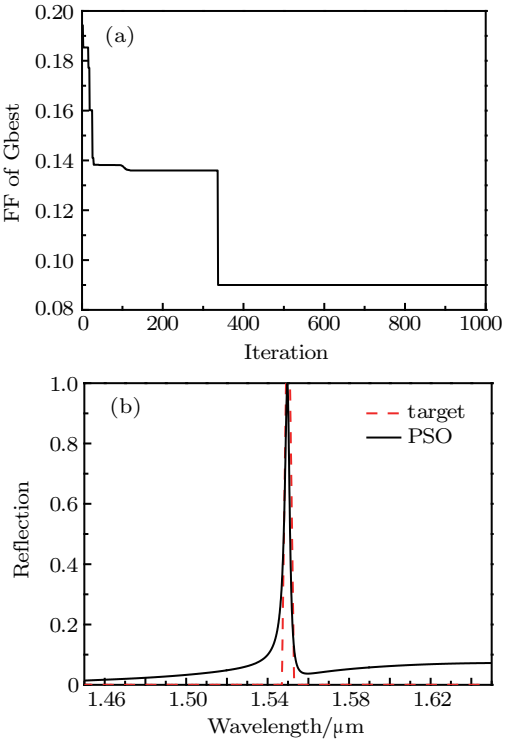


Fig. 3. (color online) (a) FF of the best particle (Gbest) versus the number of iterations for the reflection filter, and (b) reflectance spectrum of the designed filter by PSO co-plotted with the target spectrum. The incident angle is $\theta = 0°$.

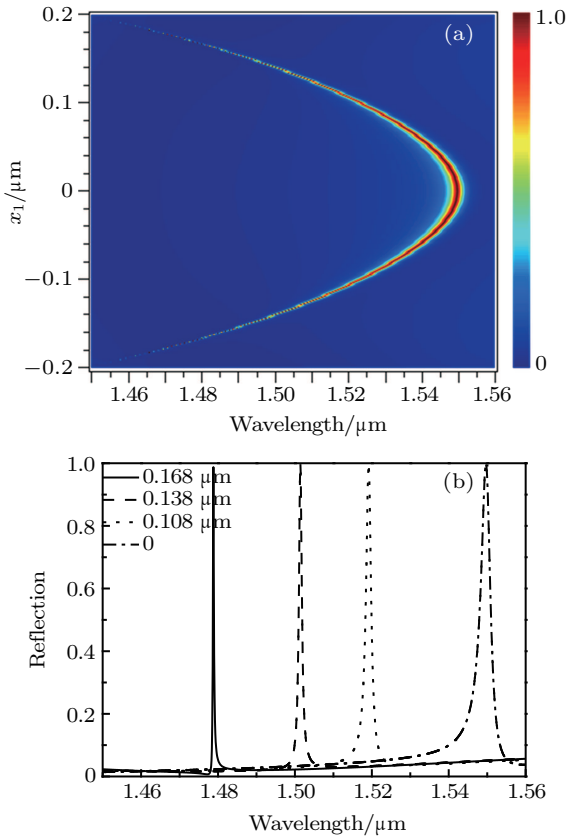


Fig. 4. (color online) (a) Color-coded map illustration of resonance tuning $R(\lambda, x_1)$ while holding $y_1 = z_1 = 0$, and (b) reflectance spectra for various values of x_1. The incident angle is $\theta = 0°$.

Figure 4 shows results of reflection spectra with F2 fraction moving in the horizontal direction. To simulate this action, x_1 parameter is set to be varied from −0.2 μm to +0.2 μm and y_1 and z_1 parameters are both assumed to be constant ($y_1 = z_1 = 0$). Resonant wavelength tuning versus x_1 variation $R(\lambda, x_1)$ is depicted in Fig. 4(a). According to this figure, the reflectance map is symmetric around ($x_1 = 0$). It means that, for instance, the physical situation for $x_1 = 0.1$ μm is the same as $x_1 = -0.1$ μm. Hence the tuning with horizontal motion varies the symmetry of the structure profile by changing x_1 parameter within the −0.2 μm–+0.2 μm. Figure 4(b) illustrates four reflectance spectra from the reflectance map in Fig. 4(a).

These reflectance spectra display fairly narrow resonances. As depicted in Fig. 4(b), the location of the resonance can be adjusted about 70 nm in the 1.48 μm–1.55 μm range, through a horizontal movement of 168 nm via MEMS actuators. Also, reflection efficiency of the shifted resonance remains constant.

In addition to the movement in the horizontal direction, the inner F2 fraction attached to the substrate could also be moved vertically via MEMS elements. Here we only treat the case of downward movement, and z_1 parameter is used to measure this movement. Figure 5 shows the reflection spectra with F2 fraction movements in the vertical direction, and x_1, y_1 parameters are assumed to be constant ($x_1 = y_1 = 0$). Figure 5(a) depicts the resonant wavelength tuning versus z_1 parameter variation $R(\lambda, z_1)$. As shown in this figure, the structure has a tunability of 100 nm in the 1.45–1.55 μm region through 435 nm of vertical movement. Four reflectance spectra for different z_1 parameters in Fig. 5(a) are shown in Fig. 5(b).

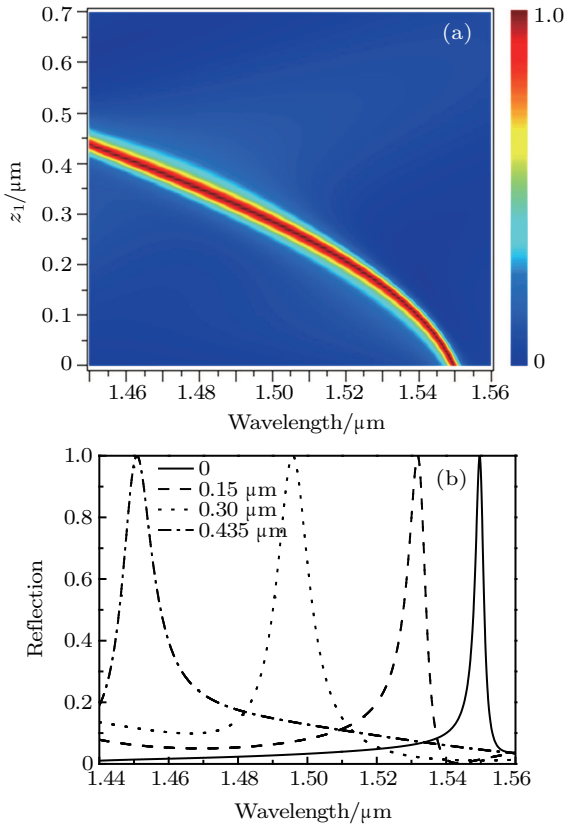


Fig. 5. (color online) (a) Color-coded map illustration of resonance tuning $R(\lambda, z_1)$ while holding $x_1 = y_1 = 0$, and (b) reflectance spectra for various values of z_1. The incident angle is $\theta = 0°$.

To study the angular sensitivity, structure responses under different values of incident angle (θ) are simulated while holding $x_1 = 0$, $y_1 = 0$, and $z_1 = 0$, and the results are illustrated in Fig. 6. According to the two-dimensional (2D) color map in Fig. 6(a), the reflectance is also symmetric around ($\theta = 0°$), that is, for example, the diffraction situation for $\theta = 10°$ is the same as for $\theta = -10°$. Figure 6(b) illustrates four reflectance spectra under incident angles of 0°, 4°, 8°, and 11° from the reflectance map in Fig. 6(a). The resonant wavelength can be tuned from 1.55 μm to 1.59 μm through about an 11° variation of incident angle. These reflectance spectra display fairly narrow resonances with high diffraction efficiency (100%).

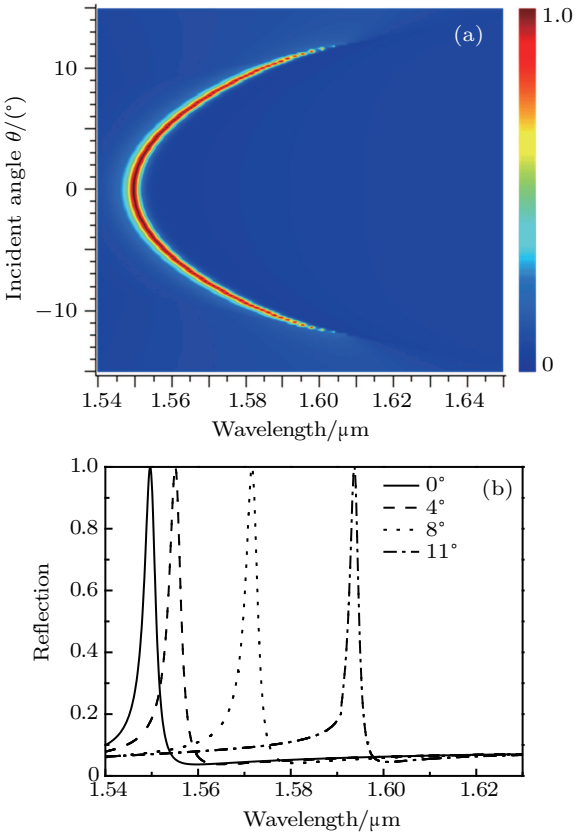


Fig. 6. (color online) (a) Color-coded map illustration of resonance tuning $R(\lambda, \theta)$ while holding $x_1 = y_1 = z_1 = 0$, and (b) reflectance spectra for various values of incident angle θ.

Since the movement (168 nm) of F2 fraction in the horizontal direction can tune the resonant wavelength from 1.48 μm to 1.55 μm as shown in Fig. 4, and about an 11° variation of incident angle can tune the resonant wavelength from 1.55 μm to 1.59 μm as depicted in Fig. 6, it is possible to achieve 110 nm of resonance tuning if we combine the two tuning strategies. At the same time, it is also possible to achieve 140 nm of resonance tuning in a 1.45–1.59 μm wavelength range, by combining a vertical motion of 435 nm (Fig. 5) and about an 11° variation of incident angle (Fig. 6).

4. Conclusions

A compact tunable GMRF in the telecommunications region near the 1550 nm wavelength is proposed in this paper. The PSO method is used to design this structure, in order to obtain optimal structural parameters. The MEMS-based physical movement of F2 fraction is achieved in the horizontal and vertical directions. The results show that the location of the resonance is shifted by about 70 nm (from 1.48 μm to 1.55 μm) and 100 nm (from 1.45 μm to 1.55 μm), with a

horizontal movement of 168 nm and a vertical movement of 438 nm, respectively. In addition, the resonant wavelength is tuned from 1.55 μm to 1.59 μm through about an 11° variation of incident angle. Therefore, this dynamic structure is a good candidate for tunable filters, by combining the MEMS-based physical movement with a variation of incident angle.

References

[1] Xu B L, Zhang D W, Huang Y, *et al.* 2014 *IEEE Photon. Technol. Lett.* **26** 231
[2] Uddin M J 2012 *IEEE Photon. Technol. Lett.* **24** 1552
[3] Zheng G G, Xu L H and Pei S X 2014 *Chin. Phys. B* **23** 034213
[4] Ma J Y and Fan Y T 2012 *Chin. Phys. B* **21** 037801
[5] Wang W, Zhu G Y, Liu Q F, *et al.* 2016 *Opt. Express* **24** 11033
[6] Sun T Y, Ma J Y and Fu X Y 2010 *Chin. Opt. Lett.* **8** 447
[7] Kikuta H, Toyota H, Yu W J, *et al.* 2004 *SPIE* **5515** 125
[8] Uddin M J 2012 *IEEE Photon. Technol. Lett.* **24** 1552
[9] Uddin M J and Magnusson R 2013 *Opt. Express* **21** 12495
[10] Sang T, Wang Y K, Li J L, *et al.* 2017 *Opt. Commun.* **382** 138
[11] Lin H A and Huang C S 2016 *IEEE Photon. Technol. Lett.* **28** 1042
[12] Wu Y, Xia Z, Wang Z, *et al.* 2012 *Opt. Commun.* **285** 2840
[13] Qian L, Zhang D, Dai B, *et al.* 2015 *Opt. Lett.* **40** 713
[14] Wang Q, Zhang D, Huang Y, *et al.* 2010 *Opt. Lett.* **35** 1236
[15] Uddin M J and Magnusson R 2013 *IEEE Photon. Technol. Lett.* **25** 1412
[16] Magnusson R and Ding Y 2006 *IEEE Photon. Technol. Lett.* **18** 1479
[17] Magnusson R and Shokooh-Saremi M 2008 *IEEE in Aerospace Conference*, March 1–8, 2008, Big Sky, MT, p. 7
[18] Gao X M, Wu T, Xu Y, *et al.* 2015 *Opt. Express* **23** 15235
[19] Shokooh-Saremi M and Magnusson R 2007 *Opt. Lett.* **32** 894
[20] Shokooh-Saremi M and Magnusson R 2014 *Opt. Lett.* **39** 6958